Available online at www.sciencedirect.com
SCIENCE DIRECT
Catalysis Today 110 (2005) 68–75
CATALYSIS TODAY
www.elsevier.com/locate/cattod

Packed bed versus microreactor performance in autothermal reforming of isooctane

Andrew R. Tadd, Benjamin D. Gould, Johannes W. Schwank *

Department of Chemical Engineering, University of Michigan, Ann Arbor, MI 48109-2136, USA

Available online 10 October 2005

Abstract

The performance of a $Ni/Ce_{0.75}Zr_{0.25}O_2$ catalyst for the autothermal reforming of isooctane is evaluated and compared using typical packed bed reactors, steel microreactors, and quartz microreactors. Microchannel reactor systems have in recent years been proposed as attractive alternatives to traditional catalytic packed bed reactors due to their improved heat and mass transfer properties. The microreactors employed in this study are comprised of stackable layers, with FeCrAlloy metal foams serving as catalyst substrate. To deploy the $Ni/Ce_{0.75}Zr_{0.25}O_2$ catalyst in the microreactors, the metal foam substrates were coated with a catalyst washcoat formulation.

Several factors are discussed that may influence the microreactor performance, with emphasis on the different contributions of heat transfer mechanisms between the active reaction zone and its surroundings, the materials of construction, and reactor aspect ratio.

Heat effects were found to be particularly important in determining performance for the steel microreactors.

Keywords: Microreactor; Autothermal; Reforming; Ceria; Nickel; Isooctane

1. Introduction

The recent interest in both industry and academia in low-temperature proton exchange membrane (PEM) fuel cells has spurred research into methods of hydrogen production that could supply a ready and sufficiently pure feed stream. Processing liquid fuels into hydrogen rich streams has been suggested as an approach possessing several advantages for portable applications in vehicles or small, distributed generators. Producing hydrogen from liquid fuels on demand eliminates the problem of hydrogen storage and allows the use of the existing liquid fuel distribution infrastructure. The challenge, however, is that a small-scale, dynamic reforming system must be developed. Current hydrocarbon reforming technology is primarily focused on methane and natural gas, and is practiced on large industrial scales under steady-state process conditions. Significant materials and engineering breakthroughs must be realized to fill the gap between traditional reforming technology and that required to complement a portable fuel cell power system.

Fuel processing breaks down liquid hydrocarbon fuels into hydrogen and carbon dioxide through a sequence of processing steps. It first uses a reformer to break the hydrocarbons into hydrogen and carbon monoxide. For solid oxide fuel cells (SOFCs), this single step is often sufficient. In order to fuel a conventional low temperature PEM fuel cell, however, the CO content must be reduced to less than 10–50 ppm. This is usually accomplished by passing the crude reformate through a CO clean-up system, comprising one or more water–gas shift reactors, where carbon monoxide is converted to carbon dioxide, producing additional hydrogen, and a preferential oxidizer, where the remaining carbon monoxide is selectively burned with oxygen or air.

Regardless of whether the goal is to supply a PEM fuel cell or an SOFC, the heart of a fuel processor is the reformer. There are three general reforming schemes that may be applied. The first is steam reforming, where the fuel is reacted with steam over a catalyst at high temperature, as shown in Eq. (1):

$$C_8H_{18} + 8H_2O \rightarrow 8CO + 17H_2, \qquad \Delta H = 1274\,\mathrm{kJ/mol} \quad (1)$$

Steam reforming has the highest hydrogen yield of all reforming options, but is highly endothermic. As such, it may

* Corresponding author. Tel.: +1 734 764 3374; fax: +1 734 763 0459.
E-mail address: schwank@umich.edu (J.W. Schwank).

0920-5861/$ – see front matter © 2005 Elsevier B.V. All rights reserved.
doi:10.1016/j.cattod.2005.09.018

operate in a heat transfer limited mode. Alternatively, partial oxidation may be applied. The fuel is burned with a sub-stoichiometric quantity of oxygen, described in Eq. (2):

$$C_8H_{18} + 4O_2 \rightarrow 8CO + 9H_2, \qquad \Delta H = -660\,\mathrm{kJ/mol} \qquad (2)$$

Partial oxidation is exothermic, so no external heat source is required. It may reach high temperatures, be difficult to control, and has the lowest hydrogen yield of the three reforming reactions. The final choice is autothermal reforming (ATR), which is in reality a combination of the first two, as shown in Eq. (3):

$$C_8H_{18} + xO_2 + (8 - 2x)H_2O \rightarrow 8CO + (17 - 2x)H_2 \qquad (3)$$

The fuel is reacted with steam and oxygen in a single reactor. Some portion of the fuel undergoes oxidation, generating heat to drive the steam reforming of the remaining fuel. ATR has an intermediate hydrogen yield, and the heat of reaction may be adjusted by varying the steam to carbon ratio (H_2O/C) and the oxygen to carbon ratio (O/C). It is also expected that this flexibility will make ATR the best choice for load following applications.

A good catalyst for ATR must possess several important characteristics. It must catalyze both hydrocarbon oxidation and reforming reactions, withstand high operating temperatures for extended periods, and have a resistance to the deposition of carbon. It is clear from the literature that base metal catalysts are capable for hydrocarbon reforming. Commercial steam reforming catalysts for the conversion of natural gas have usually been nickel supported on alumina. These catalysts, however, have suffered from coking at low steam to carbon ratios, especially for higher hydrocarbons, and so are usually promoted with various alkali compounds (K_2O, MgO) to decrease carbon deposition [1]. Ceria and doped ceria have been suggested in the literature as interesting supports for oxidation and reforming catalysts. Ceria has the ability to release oxygen and reduce its valence from Ce^{4+} to Ce^{3+} in oxygen-poor environments, then re-oxidize in oxygen-rich environments [2]. This oxygen storage ability might lead to improvements in coking resistance by promoting the oxidation of carbon deposits through the activity of the support, and a bifunctional mechanism involving the support has been proposed for *n*-butane reforming [3] and methane reforming [4]. Pino et al. reported that ceria supported platinum was capable of performing methane partial oxidation at stoichiometric ratios for 100 h with no deactivation and almost no carbon deposition [5]. Nickel supported on lanthanum-doped ceria was also active for methane partial oxidation [6]. Low nickel loadings, which retained high dispersion under reaction conditions, showed good stability and were resistant to carbon deposition. Ceria–zirconia mixed oxides, with no additional active components, were demonstrated to be active for methane oxidation [7]. The lowest light-off temperatures were obtained with $Ce_{0.75}Zr_{0.25}O_2$, which was better than either pure ceria or zirconia.

Ceria has also been used in the preparation of reforming catalysts. Pd/CeO_2, Ni/Ce–ZrO_2, and Nb doped ceria have been reported for methane reforming [8–10]. Wang and Gorte reported the use of Pd/CeO_2 for the steam reforming of *n*-butane at steam to carbon ratios of 1–2 [3]. The ceria supported catalyst was much more resistant to coking when compared to a Ni/SiO_2 catalyst, which deactivated so quickly that reaction rates could not be obtained. The same group later reported results for steam reforming of various hydrocarbons, including hexane, *n*-octane, and benzene, using Pd/CeO_2 catalysts [11]. Rates for the Pd/CeO_2 catalyst were much higher than for a Pd/Al_2O_3 catalyst that was also tested. At low conversions, Pd/CeO_2 exhibited dealkylation for toluene and ring closure for 2,4-dimethylhexane and *n*-octane, leading to cyclohexane. The cyclohexane could be dehydrogenated to give benzene over the same catalyst.

In addition to new materials, new reactor engineering approaches may be required to achieve the performance levels needed for portable fuel processor systems. In industrial steam reformers reaction rates are often heat transfer limited [1]. Microchannel reactor systems have in recent years been proposed as alternatives to traditional catalytic reactors due to their improved heat and mass transfer properties [12]. In microchannel reactors, the primary transport modes are conduction and diffusion, which are much slower than convection at common length scales. The very small dimensions used, however, result in these transport modes being faster than convection perpendicular to the flow direction. This applies more generally in metal foams. Several groups have started studying reforming and hydrogen production using microchannel devices. Reuse et al. have reported on the production of hydrogen from methanol using a thermally integrated steam reformer–combustor [13]. Park et al. have also developed a microchannel methanol steam reformer [14]. Both groups were able to obtain high conversions. The high surface area to volume ratio that leads to improved heat and mass transfer rates also leads to high heat losses to the environment. Both Reuse et al. and Park et al. report the need for electrical heat support. Furthermore, Reuse et al. indicated that the temperature behavior of their microreactor was controlled by the thermal inertia of the system. Methanol steam reforming takes place at relatively low temperatures (~240–300 °C). Thermal inertia and loss effects may be expected to be more pronounced for autothermal reformers operating at much higher temperatures. The thermal coupling of the reaction zone to the housing and the ambient environment and the choice of materials of construction will be expected to play an important role in device performance. Other outstanding questions are the interaction between heterogeneous and homogeneous chemistry at high reactor temperatures, and possible effects of reactor aspect ratio. Microchannel reactors have L/D ratios that may be very different than typical packed bed reactors.

In this work we report on the performance of a Ni/$Ce_{0.75}Zr_{0.25}O_2$ catalyst for the autothermal reforming of isooctane. Experiments using typical packed bed reactors and steel microreactors were compared. Heat effects were found to be particularly important in determining performance for the steel microreactors.

2. Experimental

2.1. Catalyst preparation

Supports and catalysts were prepared in our laboratory. The mixed oxide support, $Ce_{0.75}Zr_{0.25}O_2$, was prepared via co-precipitation. Appropriate quantities of $Ce(NO_3)_3{\cdot}6H_2O$ and $ZrOCl_2{\cdot}8H_2O$ were dissolved in stirred de-ionized water. A solution of 2 M NH_4OH was added dropwise by an HPLC pump while vigorously stirring the precursor solution. The precipitate slurry was allowed to stir overnight, then recovered by vacuum filtration. The filter cake was washed twice with de-ionized water, and then dried overnight in an oven at 110 °C. The resulting solid was crushed and calcined in air at 600 °C.

Catalysts were prepared from the mixed oxide support by impregnation with a nickel solution. Appropriate quantities of $Ni(NO_3)_2{\cdot}6H_2O$ were dissolved in ethanol, then dropped onto the support powder until it was saturated. The support was then allowed to dry. The addition and drying procedure was continued until the impregnation was completed. Following the impregnation, the catalyst was calcined in air at 600 °C. All catalysts used in this work were prepared as 10% nickel by weight, calculated as the weight of nickel divided by the weight of the nickel and the support.

2.2. Characterization

Supports and catalysts were characterized using several different techniques. Solid phases were identified using X-ray diffraction on a Rigaku rotating anode instrument and Cu Kα radiation. Physical surface area was determined using N_2 physisorption at 77 K and the single point BET method. Nickel surface area was determined by H_2 pulse chemisorption at 100 °C for selected samples.

2.3. Microreactor design

The microreactor employed a layer-based design, using FeCrAlloy metal foams as a catalyst substrate. The design and hardware is shown in Fig. 1. Each catalyst layer was placed between separation plates, which were sealed with a graphite gasket held in place by a gasket retainer. The layers were assembled and compressed between two cover plates, which included welded-in Swagelok® fittings for gas connections and sockets for four electric cartridge heaters. Each cartridge heater was capable of supplying 125 W of power. The catalyst foams were 30 mm × 30 mm, with a thickness of 600 μm. The separation layers and gasket retainers were also 600 μm in thickness. The design of the layers allows for construction of single-fluid parallel flow reactors and two-fluid parallel or counter flow reactors/heat exchangers, simply by reversing the flow directions in alternating layers. All microreactor components other than the gaskets and catalyst foams were constructed using 310 stainless steel.

Following experimentation with the steel microreactors, a separate quartz reactor was fabricated capable of holding a single catalyst foam. The quartz reactor was used in conjunction with steel microreactors to investigate the effects of heat transfer on catalyst light-off.

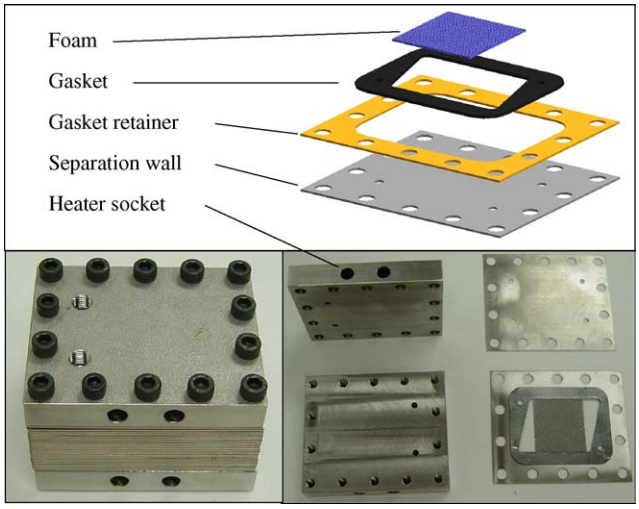

Fig. 1. Clockwise from top: exploded view of the repeating layer structure showing individual microreactor components; photograph of the fabricated components, including the cover plates with cartridge heater sockets; an assembled reactor module comprising 25 layers (overall dimensions 80 mm × 70 mm × 60 mm).

2.4. Washcoat preparation

A washcoat based on the nickel catalysts was prepared in order to deploy them in the microreactors for testing. To prepare the washcoat, the catalyst was mixed with water, polyvinyl alcohol, and a ceria–zirconia binder prepared from pure support. The mixture was ball-milled with zirconia grinding media for 48 h, resulting in a uniform slurry. Prior to washcoating, the metal foam substrates were calcined in air at 800 °C, which produces an Al_2O_3 surface layer to which the washcoat bonds. The washcoat mixture was placed in a Petri dish and stirred. Foams were submerged in the washcoat mixture, removed, placed in a quartz rack, and dried in an oven at 110 °C. Multiple washcoat additions were made, until a desired loading was achieved. Following the final drying, the rack-loaded foams were calcined in air at 600 °C to remove any remaining water and the polyvinyl alcohol. After calcination, foams had an average of about 200 mg of washcoat deposited.

2.5. Packed bed reactor studies

Catalysts and dried washcoat powders were tested for the autothermal reforming of isooctane using a fixed bed flow reactor. Samples were loaded on top of a quartz wool plug in a 12 mm o.d. quartz tube. Approximately 500 mg of catalyst was used in most runs. The quartz reactor tube was positioned in a vertically mounted electric furnace capable of reaching 1000 °C, and equipped with a temperature controller with ±1 °C accuracy. Type K thermocouples were fitted above and below the catalyst bed to measure the feed gas temperature and product gas temperature, respectively. Pure nitrogen, air, and 5% H_2 in N_2 for reduction (carried out at 600 °C for 1 h) were

metered by MKS thermal mass flow controllers. Water and isooctane were delivered by HPLC pumps (Eldex) or peristaltic pumps (Instech), and mixed with the gas flow and vaporized in a heated tubing section. Typical flowrates of isooctane were 0.6 or 0.4 ml/min (3.63×10^{-4} or 2.42×10^{-4} mol/min). Corresponding air flowrates at an O/C of 1.0 are 6.9×10^{-3} or 4.5×10^{-3} mol/min. Reaction products were passed through a stainless steel cold water condenser and then through a knockout vessel positioned in an ice bath to collect excess water and unreacted hydrocarbons. Following the knockout, gas products were analyzed by online gas chromatography (Varian CP-3800) equipped with a thermal conductivity detector using argon carrier gas, and a 10-ft Carbosphere 1000 packed column (Alltech). Mole fractions of H_2, O_2, N_2, CO, CH_4, and CO_2 in the product were determined. Conversion was calculated using the gas phase carbon containing products, CO, CH_4, and CO_2, according to the following formula:

$$X = \frac{F_{N_2,in}(y_{CO} + y_{CO_2} + y_{CH_4})_{out}}{y_{N_2,out}(8F_{C_8H_{18},in})} \times 100$$

The weight hourly space velocity reported for the various runs is calculated as follows, using catalyst weight for packed bed runs and the washcoat weight for device runs:

$$\text{WHSV} = \frac{\text{flow of reactants (g/h)}}{\text{catalyst weight (g)}}$$

2.6. Microreactor studies

Microreactors were tested using the same feed delivery, knockout, and product analysis systems as were used in packed bed studies. All microreactors were run in the single feedstream, parallel flow mode. The feed stream was passed through the electric furnace, held at 500 °C, in a stainless steel tube, and then into the microreactor. The microreactors were heated using the cartridge heaters. A rheostat controlled power to the cartridge heaters manually. The device skin temperature was measured using a K-type thermocouple.

For the experiments comparing heat effects between microreactor configurations, the feed stream was passed through only the flow reactor preheater, not the furnace, before entering the device. Product analysis was determined using the flow reactor knockout and gas chromatograph. Thermocouples were positioned in four separate locations in the device: gas inlet; gas outlet; device skin; block outlet, which was inserted through the unused second stream outlet. All thermocouples were K-type. The catalyst foams were reduced using 5% H_2 in N_2 prior to reaction.

The quartz microreactor housing was tested using the same feed and analysis setup as the steel microreactor housings. The feed preheater section was unable to reach high enough temperatures to light-off the ATR reaction. To achieve higher catalyst temperatures, a single 125 W cartridge heater was placed underneath the reactor. Power was controlled manually using a rheostat. Only three thermocouples were used: gas inlet, gas outlet, and adjacent to the cartridge heater.

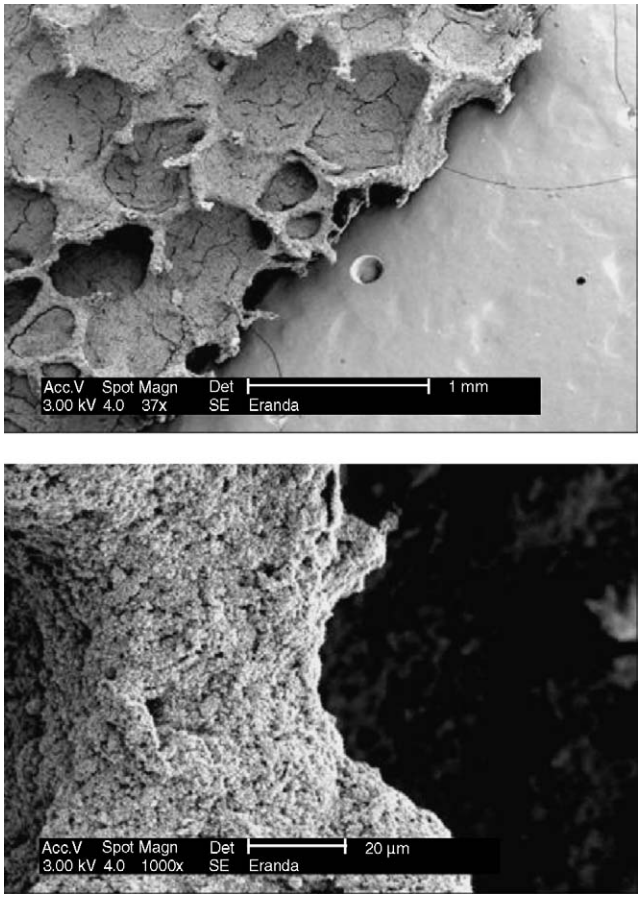

Fig. 2. An SEM image showing a metal foam which has been washcoated with catalyst, following autothermal reforming in the microreactor, at 37× magnification (top) and 1000× magnification (bottom).

3. Results and discussion

3.1. Characterization

Following preparation, X-ray diffraction indicated that the mixed oxide support, $Ce_{0.75}Zr_{0.25}O_2$, consisted of a single phase, consistent with previously published diffraction patterns [7]. X-ray diffraction of $Ni/Ce_{0.75}Zr_{0.25}O_2$ catalysts showed no change in the diffraction peaks associated with the support, but did show peaks indicating the presence of NiO. When examined after reaction, peaks associated with Ni were observed, but no NiO was indicated. Surface areas of the supports following calcination were approximately 30 m^2/g. After nickel impregnation and subsequent calcination, the fresh catalyst had a surface area of 15 m^2/g. Dispersions as measured by H_2 chemisorption were approximately 1%. Dispersion of the washcoat powders was similar to that of the catalyst. The washcoat remained on the metal foam carrier during and after reaction. Fig. 2 shows SEM images of a washcoated foam, post reaction. At the higher magnification it is apparent that the ball milling

Table 1
Summary of packed bed reactor results for autothermal reforming of isooctane

Catalyst	Inputs				Outputs					
	H_2O/C	O/C	WHSV (h^{-1})	T_{feed} (°C)	T_{exit} (°C)	H_2 (mol%)	CO (mol%)	CH_4 (mol%)	CO_2 (mol%)	X (%)
Lot A, reduced in H_2	2.0	1.0	456	525	709	26.7	10.2	nd	11.5	74
Lot A, reduced in H_2	2.0	1.0	456	600	749	27.4	12.8	nd	9.7	80
Lot A, reduced in H_2	2.7	1.3	496	525	780	22.5	8.2	0.1	11.7	88
Lot A, reduced in H_2	1.7	0.8	380	525	691	30.8	13.6	0.3	9.3	[102]
Lot A, reduced in H_2	2.1	1.0	524	525	687	31.2	16.2	0.3	7.4	87
Washcoat, reduced in H_2	1.8	0.9	357	525	612	29.3	11.0	nd	14.9	[106]
Washcoat, reduced in H_2	1.8	0.9	357	525	592	26.2	6.8	0.3	18.9	96
Lot C, no reduction	1.9	1.0	296	500	625	30.5	12.8	0.3	10.6	88
Lot D, no reduction	2.0	1.0	293	500	630	30.2	12.8	0.2	10.4	91

All catalysts are 10% $Ni/Ce_{0.75}Zr_{0.25}O_2$, washcoats are based on 10% $Ni/Ce_{0.75}Zr_{0.25}O_2$.

procedure achieved small particle sizes in the washcoat preparation.

3.2. Packed bed studies

The results from packed bed reactor studies of isooctane autothermal reforming are summarized in Table 1. Exit gas temperatures, product compositions, and isooctane conversions reported are averages over the course of each run during stable operation. Conversions for all catalyst lots and conditions are high, despite the high space velocities. The reaction is clearly running in the exothermic regime, as the exit temperatures are much higher than the feed temperatures. It is not clear whether the isooctane undergoes partial or total oxidation. If the fuel undergoes total oxidation until all the oxygen is consumed, the remaining fuel would then be steam reformed. Total oxidation would raise the bed temperature more than partial oxidation, and possibly lead to high steam reforming rates and high conversion, even at high space velocities. At an O/C of 1, however, there is enough oxygen present to partially oxidize all the fuel to CO and H_2. CO_2 and additional H_2 would then be produced through the water–gas shift reaction. Very little methane is found in the reaction products. Equilibrium product compositions for autothermal reforming of isooctane at total conversion were estimated using a Gibbs free energy minimization in ASPEN®. The results indicated that for H_2O/C of 2, O/C of 1, and temperatures above 650 °C, methane should be less than 1 mol% (dry basis).

The excess washcoat mixture from foam coating was dried and recovered as a fine powder. When tested for reforming it achieves near total conversion, although tested space velocities were lower than those examined for the fresh catalyst. The reformate produced using the washcoat had less CO and more CO_2 than in the reactions using pure catalyst. This may be a result of the lower exit temperatures and lower space velocities used in the experiment. At lower temperatures, equilibrium favors the conversion of CO to CO_2 via the water–gas shift reaction.

For several runs the reformate hydrogen content appears to be lower than would be expected for the calculated isooctane conversion. During several experiments we found the isooctane delivery pump to be inaccurate. Our calculation of isooctane conversion uses the input flowrate, which is assumed to be correct. We believe the composition results from the chromatograph to be correct, and in instances where the conversion seems too high, we believe the error lies in the fuel delivery flowrate. We have subsequently changed from a reciprocating type HPLC pump to a peristaltic pump that uses a reservoir placed on a scale. Since making this change we have had much better correspondence between exit compositions and the isooctane conversion calculated using the mass-based delivery flowrate.

The majority of experiments were undertaken after reducing the catalyst under flowing 5% H_2 in N_2. Experiments using two additional lots (C and D) of catalyst were carried out without reduction of the catalyst to investigate whether the H_2 pretreatment was necessary. The blank $Ce_{0.75}Zr_{0.25}O_2$ support alone was tested

Table 2
Summary of microreactor results for autothermal reforming of isooctane

	Inputs				Outputs					
	No. of foams used	H_2O/C	O/C	GHSV 1000 (h^{-1})	T_{device} (°C)	H_2 (mol%)	CO (mol%)	CH_4 (mol%)	CO_2 (mol%)	X (%)
Air startup	5	2	1	133	315	23.3	3.0	1.2	15.2	62
Air startup	1	2	1	770	545	21.1	6.1	0.3	13.3	58
Reduced in H_2	1	2	1	770	620	24.4	6.8	0.3	15.1	70
Reduced in H_2	1	2	1.25	770	672	23.7	6.9	0.5	16.3	76
Air startup, external insulation	1	2	1	770	698	15.4	5.4	0.6	12.3	53
Air startup, internal insulation	1	2	1	770	645	27.3	8.3	0.3	13.2	80

All catalyst foams washcoated with 10% $Ni/Ce_{0.75}Zr_{0.25}O_2$.

for autothermal reforming of isooctane. It was found to be active for oxidation, producing mainly CO_2 and only small amounts of H_2 or CO. So it may be that the unreduced catalyst is activated by the small amount of H_2 produced during oxidation over the support. Once reduced, the reforming reactions proceed and deliver a reformate similar to that obtained using a reduced catalyst. Jin et al. reported similar findings when investigating the partial oxidation of methane using a Ni/Al_2O_3 catalyst [15]. Methane conversion jumped sharply at 742 °C, producing CO, CO_2, and H_2O. After a delay, during which the nickel in the catalyst reduced, H_2 became a major product, indicating a switch from total oxidation to partial oxidation.

3.3. Microreactor studies

The results from autothermal reforming in the microreactor are summarized in Table 2. Unlike the packed bed studies, the majority of trials were carried out without pretreatment of the catalyst in H_2. It was expected that in actual applications, the ATR catalyst would need to operate without pretreatment, and so the experimental approach was adjusted accordingly. For the runs reported in Table 2, only the overall device temperature was measured, so inlet and exit gas temperatures are unavailable. Also of note are the higher space velocities used in testing the microreactors. This is a result of the small amount of catalyst loaded on each foam carrier. Even at these high space velocities, significant conversions are achieved. When the catalyst is reduced in situ the isooctane conversion increases from about 60 to 70 to 75%. Two general trends are apparent, however, when device performance is compared to the results obtained from packed bed studies. First, the isooctane conversions are generally much lower. Second, the reformate contains less CO and more CO_2. It may be that total oxidation proceeds in the microreactor, but the higher space velocity or a lower bed temperature downstream of the oxidation zone prevents the reforming reaction from reaching completion. The lower steam reforming rate would lead to lower production of CO. The apparent increase in CO_2 may simply be a result of the lower hydrogen concentration and the lower dilution of CO_2 produced via oxidation at the reactor entrance. This difference in CO/CO_2 ratio at first appears to indicate an equilibration of the water–gas shift reaction, but when the equilibrium constants are calculated from the experimental data, both the device and packed bed runs are away from equilibrium.

Several factors may have an effect on the microreactor performance. One is the heat transfer between the active reaction zone and its surroundings. In packed bed studies, the catalyst reaches extremely high temperatures, and it transfers heat to its surroundings (the electric furnace), primarily by radiation. In the microreactor, the catalyst and the gas stream are in close contact with a highly conductive metal housing. This housing may limit the ultimate temperature achieved in the reaction zone, lowering the reforming reaction rate. A further set of experiments was undertaken to determine what role heat effects might play in the microreactor performance.

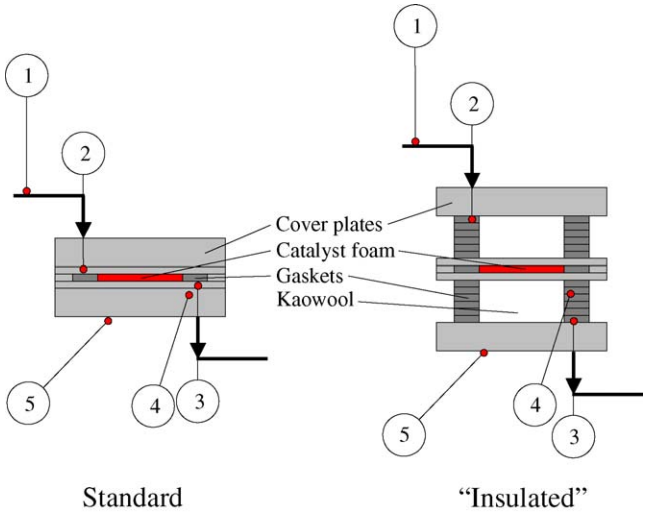

Fig. 3. Schematic representation of the standard microreactor and the "insulated" microreactor used for light-off studies. Thermocouples: (1) inlet heat tracing; (2) gas inlet; (3) gas outlet; (4) block outlet; (5) device skin.

3.4. Investigation of heat effects

Two different microreactor arrangements, described schematically in Fig. 3, were prepared and tested against each other for isooctane reforming. The first consisted of a standard microreactor with additional thermocouples. In the second "insulated" configuration, extra gaskets were added between the catalyst layer and the cover plates, producing cavities on each side of the catalyst. These cavities were filled with Kaowool insulation to reduce the conduction heat losses out of the reaction zone. Both microreactors were wrapped in Kaowool to add additional external insulation. The catalyst was reduced in the device under 5% H_2 in N_2 at 500 °C, then the device was brought to 300 °C, and reactant feed was started. Increasing the voltage to the embedded cartridge heaters gradually increased the device temperatures. The exit gas was analyzed using the gas chromatograph and the isooctane conversion calculated.

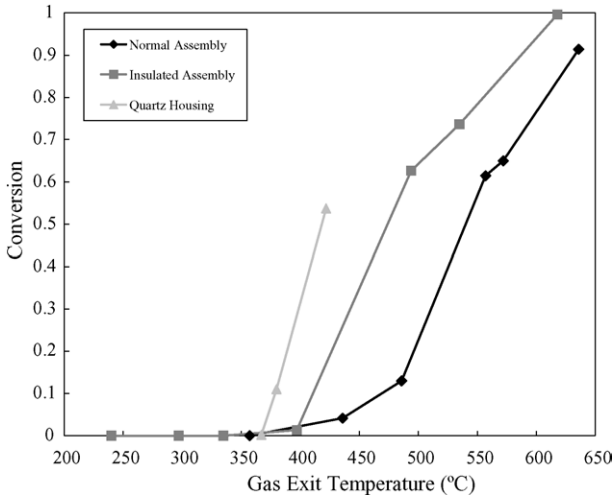

Fig. 4. Light-off curves for ATR of isooctane, $H_2O/C = 2$, $O/C = 1$, GHSV = 560,000 h^{-1}, using single foam washcoated with 10% $Ni/Ce_{0.75}Zr_{0.25}O_2$ in different reactor assemblies.

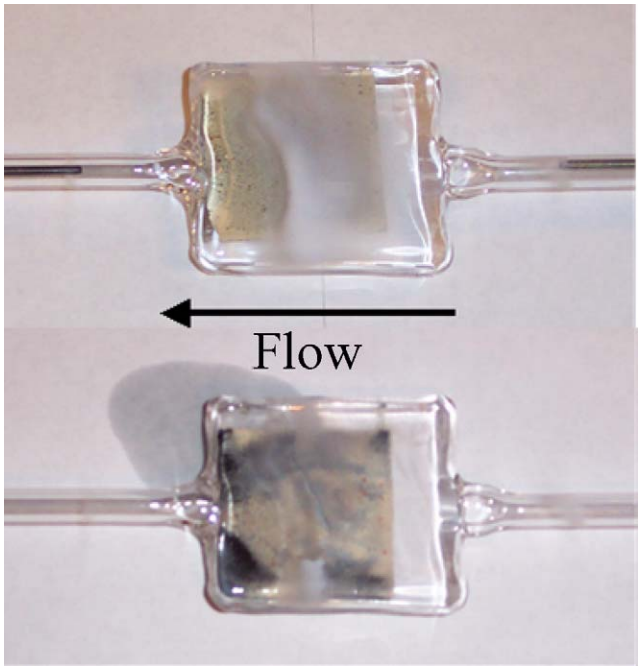

Fig. 5. Quartz reactor housing loaded with a single catalyst foam prior to reduction (top) and after reaction (bottom).

The light-off curves shown in Fig. 4 were obtained by plotting the conversion of isooctane against the measured gas exit temperature. It can be seen that the ''insulated'' microreactor achieves light-off at lower temperatures than the standard assembly. In light of this result, a quartz reactor housing capable of holding one catalyst foam was constructed (Fig. 5). This was tested under the same protocol as the steel microreactors, and was found to achieve light-off at lower temperatures than the two microreactors assembled with steel housings. The ultimate isooctane conversion in the quartz housing was limited to about 50%, which may be due to reactant bypassing. The quartz reactor was fabricated with a channel thickness of approximately 1 mm, larger than the 600 μm in the steel microreactor. As can be seen in Fig. 5, there was also additional space to either side of the catalyst foam.

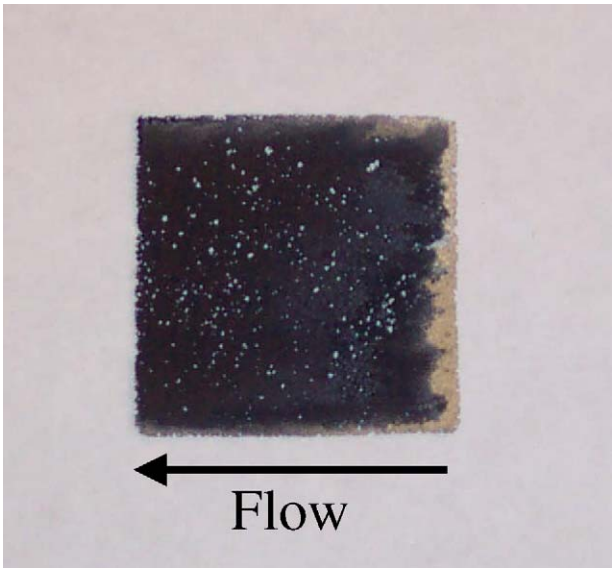

Fig. 6. Picture of a catalyst foam after ATR of isooctane in the normally assembled microreactor.

An examination of the catalyst foams recovered after reaction shows two distinct regions (Fig. 6). At the feed side of the foam, the catalyst appears similar to unreduced catalyst. It is likely that this is the oxidation region of the reactor and appears to be confined to the first 10% of the bed length. This appearance can be contrasted with catalyst foam used in the quartz housing, shown in Fig. 5. The coloration associated with the oxidation zone is much more extensive in the quartz reactor. This may indicate that the catalyst foam maintained a higher temperature in the quartz housing than in the steel housing.

4. Conclusions

Catalysts based on nickel supported on a ceria–zirconia mixed oxide are active for the autothermal reforming of isooctane without significant coking. High conversions can be achieved, even at high space velocities, and the product composition approaches equilibrium predictions. The catalyst could be successfully deployed as a washcoat in microreactor devices. Heat loss from the catalyst bed was found to have a significant effect on device performance. Microreactors that operated with lower environmental losses achieved lower reaction light-off temperatures. For high temperature reactions, the consideration of thermal isolation, either through design or materials selection, of microreactors will play an important role in achieving desired performance. Further investigation of the effects of reactor aspect ratio on performance is probably warranted.

Acknowledgements

The authors wish to acknowledge the U.S. Department of Energy for financial support under Project Grant DE-FC04-02AL67630, Prof. Jun Ni and Gap-Yong Kim of the Mechanical Engineering Department for design and fabrication of the steel microreactors, and Master Glassblower Harald Eberhart for construction of the quartz reactor housing. Eranda Nikolla and Deshpremy Mukhija were most helpful in obtaining SEM images.

References

[1] J.R. Rostrup-Nielsen, Catalysis: science and technology, Catalytic Steam Reforming, vol. 5, Springer-Verlag, 1984 (Chapter 1).
[2] A. Holmgren, D. Duprez, B. Andersson, J. Catal. 182 (1999) 441.
[3] X. Wang, R.J. Gorte, Catal. Lett. 73 (2001) 15.
[4] W.-S. Dong, K.-W. Jun, H.-S. Roh, Z.-W. Liu, S.-E. Park, Catal. Lett. 78 (2002) 215.
[5] L. Pino, V. Recupero, S. Beninati, A.K. Shukla, M.S. Hegde, P. Bera, Appl. Catal. A 225 (2002) 63.
[6] T. Zhu, M. Flytzani-Stephanopoulos, Appl. Catal. A 208 (2001) 403.

[7] S. Pengpanich, V. Meeyoo, T. Rirksomboon, K. Bunyakiat, Appl. Catal. A 234 (2002) 221.
[8] R. Craciun, W. Daniell, H. Knözinger, Appl. Catal. A 230 (2002) 153.
[9] W.-S. Dong, H.-S. Roh, K.-W. Jun, S.-E. Park, Y.-S. Oh, Appl. Catal. A 226 (2002) 63.
[10] E. Ramirez-Cabrera, N. Laosiripojana, A. Atkinson, D. Chadwick, Catal. Today 78 (2003) 433.
[11] X. Wang, R.J. Gorte, Appl. Catal. A 224 (2002) 209.
[12] V. Hessel, St. Hardt, H. Löwe, Chemical Micro Process Engineering: Fundamentals, Modelling and Reactions, Wiley-VCH, Weinheim, 2004 .
[13] P. Reuse, A. Renken, K. Haas-Santo, O. Görke, K. Schubert, Chem. Eng. J. 101 (2004) 133.
[14] G.-G. Park, D.J. Seo, S.-H. Park, Y-G. Yoon, C.-S. Kin, W.-L. Yoon, Chem. Eng. J. 101 (2004) 87.
[15] R. Jin, Y. Chen, W. Li, W. Cui, Y. Ji, C. Yu, Y. Jiang, Appl. Catal. A 201 (2000) 71.